Author Manuscript:
Published in final edited form as:
Journal of Electron Spectroscopy and Related Phenomena 190 (2013) 127–136.
https://doi.org/10.1016/j.elspec.2013.08.011

Calculations of Mean Escape Depths of Photoelectrons in Elemental Solids Excited by Linearly Polarized X-rays for High-Energy Photoelectron Spectroscopy

S. Tanuma[a,*], H. Yoshikawa[a], H. Shinotsuka[b], and R. Ueda[a]

[a]National Institute for Materials Science, 1-2-1 Sengen, Tsukuba, Ibaraki 305-0047, Japan

[b]Advanced Algorithm & Systems, Co. Ltd., Ebisu IS Bldg. 7F, Ebisu 1-13-6, Shibuya, Tokyo 150-0013, Japan

We have calculated mean escape depths (MEDs, D) of photoelectrons from Si, Cu, and Au excited by linearly polarized X-rays over the 50 to 10,000 eV energy range for high-energy photoelectron spectroscopy. These calculations were done with Monte Carlo methods using the values of electron inelastic mean free paths λ that were calculated by the relativistic full Penn algorithm and the Dirac-Hartree-Fock atomic potential for elastic scattering of electrons. In order to know the dependence of MED on the asymmetry parameter β and the emission angle θ, we calculated MEDs for β= -1 to β= 2 (by 0.5 steps) and θ =0° to θ=80° (with respect to the surface normal). The resulting MED values increase as the β values decrease over the 50 to 10,000 eV energy range. We also found that the values of $D/\lambda\cos\theta$ are approximately constant to within 10% for a given value of θ and for energies over 1000 eV (except for the condition of β=-1) over a range of emission angles (typically 0° - 40° or 60°). We also found that the energy dependence of the ratios $D/\lambda\cos\theta$ at emission angle θ =0° can be expressed by the Jablonski-Powell predictive equation over the 50 to 10,000 eV energy range.

Finally, we have obtained a predictive MED equation that could be applied to the wide range of experimental conditions that are used in high-energy XPS with synchrotron radiation.

KEYWORDS: high-energy photoelectron spectroscopy, mean escape depth, linearly polarized X-rays, asymmetry parameter

*Corresponding author. Tel.;+81 29 860 4801 Fax.:+81 29 860 4983; E-mail address: tanuma.shigeo@nims.go.jp (S. Tanuma).

Author Manuscript:
Published in final edited form as:
Journal of Electron Spectroscopy and Related Phenomena 190 (2013) 127–136.
https://doi.org/10.1016/j.elspec.2013.08.011

1. Introduction

The mean escape depth (MED) of photoelectrons is an essential quantity for X-ray variable electron spectroscopy. It is a convenient measure of surface sensitivity in X-ray photoelectron spectroscopy (XPS) because it is a function of both the specimen and the measurement conditions.[1,2] If the effects of elastic electron scattering are neglected, the MED is equal to the electron inelastic mean free path (IMFP) multiplied by the cosine of the emission angle with respect to the surface normal. In general, elastic scattering of electrons cannot be neglected because it can appreciably modify the contributions to signals arising from different depths. The MED must, then, be calculated from emission depth distribution function (EDDF), as shown later.

Formerly, the photoelectron signal attenuation has been frequently expressed by the IMFP, attenuation length, effective attenuation length (EAL), or MED. Now, these quantities have separate specific meanings. ISO 181115[3] defines these quantities as follows:

Definition of IMFP: average distance that an electron with a given energy travels between successive inelastic collisions.

Definition of attenuation length: quantity l in the expression $\Delta x/l$ for the fraction of a parallel beam of specified particles or radiation removed in passing through a thin layer Δx of a substance in the limit as Δx approaches zero, where Δx is measured in the direction of the beam.

NOTE 1 The intensity or number of particles in the beam decays as $\exp(-x/l)$ with the distance x.

NOTE 2 For electrons in solids, the behaviour only approximates to an exponential decay due to the effects of elastic scattering. Nevertheless, for some measurement conditions in AES and XPS, the signal intensity may depend approximately exponentially on path length, but the exponential constant (the parameter l) will then normally be different from the corresponding inelastic mean free path. Where that approximation is valid, the term effective attenuation length is used.

Author Manuscript:
Published in final edited form as:
Journal of Electron Spectroscopy and Related Phenomena 190 (2013) 127–136.
https://doi.org/10.1016/j.elspec.2013.08.011

Definition of EAL: parameter which, when introduced in place of the inelastic mean free path into an expression derived for AES and XPS on the assumption that elastic scattering effects are negligible for a given quantitative application, will correct that expression for elastic scattering effects.

NOTE 1 The effective attenuation length may have different values for different quantitative applications of AES and XPS. However, the most common use of effective attenuation length is in the determination of overlayer-film thicknesses from measurement of the changes of overlayer and substrate Auger-electron or photoelectron signal intensities after deposition of a film or as a function of emission angle. For emission angles of up to about 60° (with respect to the surface normal), it is often satisfactory to use a single value of this parameter. For larger emission angles, the effective attenuation length can depend on this angle.

NOTE 2 Since there are different uses of this term, it is recommended that users specify clearly the particular application and the definition of the parameter for that application (e.g. by giving an equation or by providing a reference to a particular source).

Definition of MED: average depth normal to the surface from which the specified particles or radiation escape as defined by

$$D = \frac{\int_0^\infty z\phi(z,\theta)dz}{\int_0^\infty \phi(z,\theta)dz} \quad (1)$$

where $\phi(z,\theta)$ is the emission depth distribution function (EDDF) for depth z from the surface into material and for angle of emission θ with respect to the surface normal.

The values of D for XPS have been calculated by Monte Carlo simulations and by solving the transport equation with Al or Mg K_α X-ray sources [4,5,6]. However, few data have been reported over a wide energy range (up to 10 keV) with a linearly polarized X-ray source which is a typical condition for high-energy X-ray photoelectron spectroscopy. Consequently, we have calculated values of D for the 50 to 10,000 eV kinetic energy range of photoelectrons using Monte Carlo methods for Si, Cu, and Au using linearly polarized X-rays. We report the energy and dipole parameter or

Author Manuscript:
Published in final edited form as:
Journal of Electron Spectroscopy and Related Phenomena 190 (2013) 127–136.
https://doi.org/10.1016/j.elspec.2013.08.011

asymmetry parameter dependence of *D* over this wide energy range.

2. Calculation

2.1 Mean Escape Depth

In the straight-line path approximation (SLA) [2] that ignores the electron elastic-scattering effect in solids, the EDDF can be described as [7]

$$\phi_{SLA}(z,\theta) = W(\beta,\psi)\exp(-z/\lambda\cos\theta) \quad (2)$$

where the normalized photoelectric cross section, W, is a function of ψ, the angle between the X-ray direction and the photoelectron emission direction (when a non-polarized X-ray beam is used), and β, the asymmetry parameter (or dipole parameter) that describes the anisotropic photoelectron emission distribution.

Then, in the SLA model, the MED can be obtained from Eq. (2) based on the definition given in Eq. (1). The MED of the detected XPS signal is given simply by

$$D = \lambda\cos(\theta) \quad (3)$$

where λ is the IMFP and θ is the electron emission angle with respect to the surface normal. This simple relation is the basis of much work that aims to obtain composition-versus-depth information using angle-resolved XPS (ARXPS).

However, it has been established that elastic scattering can appreciably modify the contributions to the signal arising from different depths, which means the EDDF cannot be expressed by a simple exponential decay function. Therefore, the MED, D, will be calculated from the EDDF based on the definition shown in Eq. (1), instead of the simple relation between IMFPs and detection angles as shown above. Furthermore, the anislastic scattering effects. Therotropy of photoemission caused by linearly polarized X-rays affects the EDDF due to eefore, we calculated MEDs of Si, Cu, and Au as a function of depth z, emission angle θ, and asymmetry parameter β using equation (4) with Monte Carlo methods over the 50 to 10,000eV energy range using relativistic IMFPs and a Dirac-Hartree-Fock atomic potential [8] for elastic scattering.

Author Manuscript:
Published in final edited form as:
Journal of Electron Spectroscopy and Related Phenomena 190 (2013) 127–136.
https://doi.org/10.1016/j.elspec.2013.08.011

$$D = \frac{\int_0^\infty z\phi(z,\theta,\beta)dz}{\int_0^\infty \phi(z,\theta,\beta)dz} \quad (4)$$

The angular distribution of the photoelectron produced from linearly polarized X-rays, $I(\Theta)$, can be described by the following equation [9].

$$I(\Theta) = \frac{\sigma}{4\pi}\left[1+\frac{\beta}{2}\left(3\cos^2\Theta-1\right)+\left(\gamma\cos^2+\delta\right)\sin\Theta\cos\Phi\right] \quad (5)$$

where σ is the photo ionization cross-section, β is the asymmetry parameter, Θ is the emission angle of the photoelectron from the incident electric field vector direction of the linearly polarized X-rays, Φ is the angle between the photon direction (on X-Z plane) and the plane passing through the z axis and the photoelectron direction (on Y-Z plane) . The γ and δ are the nondipole parameters. These nondipole parameters become important at higher energy (> 5 keV).[10]

The geometry between the incident linearly polarized X-ray and detector is shown in Figure 1. This configuration is typical for XPS coupled with synchrotron radiation. From this figure, we can obtain the following equation [11,12] from Eq.(5) for the angular distribution of the photoelectron since the contribution of the third term in the equation is negligible small because the value of $\cos(\Phi)$ is very small in this condition ($\Phi = 90^\circ \sim 95^\circ$).

$$I(\Theta) = \frac{\sigma}{4\pi}\left[1+\frac{\beta}{2}\left(3\cos^2\Theta-1\right)\right] \quad (6)$$

We calculated EDDFs over the 50 to 10,000eV energy range with MC methods using various asymmetry parameters (β= -1 to 2 (0.5 step)) for Si, Cu, and Au in order to investigate the asymmetry parameter dependence on their MEDs. We performed the calculations with emission angles of 0 to 80 degrees with respect to the surface normal. The solid angle of the detector was ±5 degrees.

Author Manuscript:
Published in final edited form as:
Journal of Electron Spectroscopy and Related Phenomena 190 (2013) 127–136.
https://doi.org/10.1016/j.elspec.2013.08.011

2.2 Inelastic Mean Free Paths

The inelastic mean free path is the most important parameter in the MC calculations of EDDFs. Tanuma et al. calculated IMFPs for the 50–2,000 eV and 50–30,000 eV energy ranges in over 60 materials from their energy loss functions using the non-relativistic full Penn algorithm (FPA) (for energies <200 or <300 eV) and the single-pole approximation.[13,14,15,16,17] In our research we have used the IMFP values of Si, Cu, and Au over the 50 to 10 000 eV energy range that were calculated with the relativistic FPA [18] from their energy loss functions. The details of the calculation and the analysis of IMFPs will be published elsewhere.

3. Results and Discussion

3.1 Mean Escape Depth

The MED results at emission angle θ=0° for the three elemental solids with various asymmetry parameters are shown in Figure 2 as a function of electron energy between 50 and 10,000 eV together with their IMFPs. The plots of MEDs in the figures show similar dependences on the electron energy over all energy ranges except for β=-1. We also note that the energy dependencies of the MEDs are quite different from that of the IMFPs. The MEDs for the three elemental solids (except for the β=-1 condition) are smaller than their corresponding IMFPs due to elastic-scattering effects.

It is remarkable that the MED values with β=-1 for all three elemental solids are larger than their corresponding IMFPs in the high-energy region (>200 eV for Si, >2000 eV for Cu, and >3000 eV for Au). This result indicates that multiple elastic scattering is essential for this condition. If we ignore the elastic-scattering effect (SLA model) when the angle between the detector and the linearly polarized X-ray electric field vector is only 5 degrees, the detected signal is very weak using this experimental configuration, as shown in Fig. 1, since the photoelectron emission is anisotropic. We could not detect photoelectrons at Θ=0 with the β=-1 condition in the SLA model. On the other hand, elastic-scattering can appreciably modify the contributions to the signals arising from different depths and thus the MED [19,20,21]. We can then detect photoelectrons due to elastic-scattering under these measurement conditions. The

Author Manuscript:
Published in final edited form as:
Journal of Electron Spectroscopy and Related Phenomena 190 (2013) 127–136.
https://doi.org/10.1016/j.elspec.2013.08.011

EDDFs at β=-1 are not simple exponential decay functions and have maxima as shown in Fig.3. Shinotsuka et al. also reported the same tendency of an EDDF for Fe that was calculated from a first-principles calculation [22].

In Fig. 3, we see that the EDDFs (except for β=-1) for Cu and Au show approximately the same exponential decay curves and that their slopes diverge similarly from the SLA model (solid line) due to the elastic-scattering effect. In Fig. 3(a), the EDDFs (except for β=-1) are in good agreement with the SLA model because the elastic-scattering effect is very weak for Si at 5000 eV (IMFP, λ= 8.92 nm << transport mean free path, λ_{tr} =190.2 nm).

3.2 Effect of the asymmetry parameter

From Fig. 2, we see that, over the 50 to 10,000 eV energy range, the MED values increase as the asymmetry parameter β is decreased. We show plots of the ratio $D(\beta)/D(\beta=0)$ as a function of electron energy in Fig. 4(a-c) in order to demonstrate the effect of the asymmetry parameter on the MED. We see large energy dependences in the plots of $D(\beta=-1)/D(\beta=0)$ for Si, Cu, and Au. However, with the exception of the β=-1 condition, the plots are approximately constant over the 50–10,000 eV energy range. The relative standard deviations of the ratios $D(\beta)/D(\beta=0)$ at $-0.5 \leq \beta \leq 2.0$ are less than 2.1% for these elemental solids. These indicate that the influence of the elastic-scattering effect on the asymmetry parameter is small in this condition.

Next, we fit the plots of the average $D(\beta)/D(\beta=0)$ values as a function of the asymmetry parameter in the $-0.5 \leq \beta \leq 2.0$ range as shown in Fig. 4(d). The resulting equation is

$$f(\beta) = \frac{D(\beta)}{D(\beta=0)} = 1.00 - 0.102\beta + 0.0577\beta^2 - 0.0133\beta^3 \qquad (7)$$

where $-0.5 \leq \beta \leq 2.0$. The accuracy or reliability of the above equation is limited because the sampling size for the calculation is small. However, Fig. 4 contains MED results for a wide range of atomic numbers (Si, Cu, and Au) and electron energies. We will discuss the magnitudes of elastic-scattering effects for these conditions later.

Then, we may conclude the elastic-scattering effect on the β is small as suggested above.

Author Manuscript:
Published in final edited form as:
Journal of Electron Spectroscopy and Related Phenomena 190 (2013) 127–136.
https://doi.org/10.1016/j.elspec.2013.08.011

As such, we believe Eq. (7) can be used to estimate the MED dependence on the symmetry parameter in practical use.

3.3 Dependence of MED on emission angle

Figs. 5, 6, and 7 show the emission angle dependence of the MED results for Si, Cu, and Au from Monte Carlo simulations with β = -1.0, 0.0, 1.0, and 2.0 at 100, 1000, 10000 eV. It is convenient to plot the MED results in the form $D/\lambda\cos\theta$ as this ratio would be unity if elastic scattering effects were negligible. Deviations from unity in the ratio in Figs. 5–7 indicate the significance of elastic photoelectron scattering. While the $D/\lambda\cos\theta$ vs. emission angle curves clearly show a dependency on β values, similar trends are observed for each element.

At θ = 0° we see the ratios $D/\lambda\cos\theta$ are smaller than 1.0 for the three elemental solids except β = -1. The values of $D/\lambda\cos\theta$ become large according to the increase of photoelectron energy over θ = 0 - 70°. These results indicate that the elastic-scattering effect becomes important for low energy photoelectron and at high emission angles.

On the other hand, the values of $D/\lambda\cos\theta$ with β=-1 at θ= 0°and 10000 eV for three elemental solids are larger than unity. We also see the values of $D/\lambda\cos\theta$ decrease according to the increase of emission angles over 0 - 40° or 0 - 50° for three elemental solids. These phenomena must be due to the strong anisotropy of photoelectron emission and the strong multiple elastic-scattering effects of emitted photoelectrons as stated in 3.1. Then, we see the non-exponential decay on EDDF with β=-1 as shown in Fig.3. Fo the β=-1 condition, we could not identify any approximately constant region within the $D/\lambda\cos\theta$ curves. In this condition, we could not carry out angle-resolved XPS measurements.

Figure 8 show the normalized MED values , $D(\theta)/D(\theta=0)\cos\theta$, as a function of emission angles at β = 0, 1, and 2. Form these figures, we see the values of $D(\theta)/D(0)\cos\theta$ increase substantially for more grazing emission angles. The sensitivity of the tendency depends on the photoelectron energy and asymmetry parameter values. The $D(\theta)/D(0)\cos\theta$ values increase rapidly as the photoelectron energy decreases and the asymmetry parameter increases. For example, $D(\theta)/D(\theta=0)\cos\theta$ values for 70° can be

Author Manuscript:
Published in final edited form as:
Journal of Electron Spectroscopy and Related Phenomena 190 (2013) 127–136.
https://doi.org/10.1016/j.elspec.2013.08.011

over 1.5 compared to the values for emission angles between 0° and 30° at 100 eV and β =2 in Au as shown in Fig. 8.

Figure 8 also shows that the values of $D(\theta)/D(0)$ cos θ with β=0 are approximately constant to within 10% for the three elements over a wide emission angle range of 0°–60°, at energies over 1000 eV. The approximately constant range of the values, $D(\theta)/D(0)$ cos θ, become narrow due to the increase of β value and decrease of electron energy. Then, it is recommended that the applicable emission angle range for ARXPS is 0°– 40° with $0 \leq \beta \leq 2$ conditions when photoelectron energies are over 1000 eV. At the liming condition $\beta \approx 0$ (with photoelectron energies over 1000 eV), we could carry out ARXPS measurements over a wider emission angle range (0°–60°). For the condition of $\beta \approx -1$, or at photoelectron energies ≤ 100 eV, ARXPS should not be used for practical analysis.

3.4 Dependence of MED on electron energy.

We show the dependence of MEDs on photoelectron energy in Fig. 9. The $D/\lambda\cos(0)$ ratios are plotted as a function of electron energy together with the calculated values (solid line) from an empirical equation proposed by Jablonski and Powell [23]. The solid lines are calculated from

$$\frac{D}{\lambda\cos(\theta)} = 1 - 0.736\omega \qquad (8)$$

where ω is the single-scattering albedo that is the ratio of the IMFP, λ, to the sum of the IMFP and the transport mean free path (TMFP, λ_{tr}). The ω parameter is a convenient measure of elastic-scattering effects in XPS. If elastic-scattering is negligibly small ($\lambda_{tr} >> \lambda$ and $\omega \rightarrow 0$), the SLA becomes valid. In general, ω is a multi-valued function against electron energy, as shown in Fig. 9(d). For example, in Au (Fig. 9(d)), two or three electron energies give the same ω value over the range $0.2 < \omega < 0.35$.

The TMFP is defined as the average distance that an energetic particle must travel before its momentum in its initial direction of motion is reduced to 1/e of its

Author Manuscript:
Published in final edited form as:
Journal of Electron Spectroscopy and Related Phenomena 190 (2013) 127–136.
https://doi.org/10.1016/j.elspec.2013.08.011

initial value by elastic scattering alone.[3] The TMFPs can be calculated from the corresponding values of the transport cross section (TCS) σ_{tr} as follows:

$$\sigma_{tr} = 2\pi \int_0^{\pi} (1-\cos\alpha) \frac{d\sigma_{el}}{d\Omega} \sin\alpha \, d\alpha \quad (9)$$

We calculated the TCSs for Si, Cu, and Au from Eq. (9) using DCSs from the Dirac-Hartree-Fock potential.[8]

From Fig. 9 (a–c), we see that the ratios D/λ are smaller than unity, except for the β =-1 condition. The deviations of D/λ from unity in the figures indicate the significance of elastic-scattering effects. Furthermore, we see that these deviations are not constant and show a clear dependence on photoelectron energy.

In Fig. 9 (a–c), the Jablonski-Powell predictive formula, however, gave the same electron-energy dependencies for the three elemental solids that have wide values of the single-scattering albedo as shown in Fig. 9(d).

The Jablonski-Powell equation was obtained from analyses of the MEDs of 16 photoelectron lines and 9 Auger-electron lines of five elemental solids and four inorganic compounds (energy range: 61 eV–1739 eV, asymmetry parameter range: $0 \leq \beta \leq 2.0$) based on the general EDDF expression for unpolarized X-rays of Tilinin et al. and Jablonski et al. [24,25] that was obtained from solution of the kinetic Boltzmann equation within the transport approximation.

As stated above, the Jablonski-Powell predictive equation for MEDs gave larger values than those of our calculations over the 50 to 10,000 eV energy range for these three elemental solids with the same asymmetry parameter values ($0 \leq \beta \leq 2.0$). This discrepancy must be due to the differences between the two calculation methods: the transport equation and the MC method as well as the effects of X-ray polarization.

The effect of X-ray polarization (linearly polarization and unpolarized) may be estimated at $\theta = 0°$ that was used in Fig.9. In this case, the angular distribution of linearly polarized X-ray can be obtained from eq.(6) with $\Theta = 5°$. On the other hand, the angular distribution of photoelectron emission with unpolarized X-rays can be described as

Author Manuscript:
Published in final edited form as:
Journal of Electron Spectroscopy and Related Phenomena 190 (2013) 127–136.
https://doi.org/10.1016/j.elspec.2013.08.011

$$I(\alpha)=\frac{\sigma}{4\pi}\left[1+\frac{\beta}{2}\left(\frac{3}{2}\sin^2\alpha-1\right)\right] \quad (10)$$

where α is the angle between the photon direction and the photoelectron emission and α = 95° in this configuration (Fig.1). Then, the ratio of photoemission distribution at θ=0 can be described as $I(\Theta=5^\circ)_{polarized}\Big/I(\alpha=95^\circ)_{no-polarized}\approx 1+\beta\Big/1+\beta/4$. Then, the effect of anisotropy of photoemission with the linearly polarized X-rays is stronger than that with unpolarized X-rays except β= 0. However, it is rather difficult to know the general tendency of the effect of X-ray polarization at $\theta\neq0$ because the angle Θ varies from 5° to 95° and α varies 90° to 95° according to the detection angle for ARXPS measurement conditions.

We show the dependency of the MED results on the single-scattering albedo in Fig. 10. We see the Jablonski-Powell equation gives reasonable values for the MED results. The values of $D/\lambda\cos\theta$ at θ=0 for the three elemental solids are, however, slightly smaller than those obtained from the Jablonski-Powell equation. In the region ω >0.3 for Au, the ratios are different from the other elements. These differences must be caused by strong elastic-scattering effect of electrons from the high atomic number element.

The plots of the $D/\lambda\cos\theta$ ratios could be expressed by the following equation that is a modification of the Jablonski-Powell equation:

$$\frac{D}{\lambda\cos(\theta)}=0.981(1-0.736\omega)\ , \qquad 0.6\geq\ \omega>0.02 \quad (10)$$

This result is plotted as the solid line in Fig. 9. The relative RMS deviation of the fit was 2.0 %, which was calculated as

$$RMS(\%)=100\times\sqrt{\sum\left(\frac{f_i^{fit}}{f_i^{MC}}-1\right)^2\Big/n} \quad (11)$$

Author Manuscript:
Published in final edited form as:
Journal of Electron Spectroscopy and Related Phenomena 190 (2013) 127–136.
https://doi.org/10.1016/j.elspec.2013.08.011

where f corresponds to $D/\lambda \cos\theta$.

Finally, the MED values calculated by MC calculations in this study can be fitted with the following expressions.

$$D = g(\beta) \times 0.981(1 - 0.736\omega)\lambda \cos\theta \tag{12a}$$

$$g(\beta) = 1.00 - 0.102\beta + 0.0577\beta^2 - 0.0133\beta^3 \tag{12b}$$

where $-0.5 \le \beta \le 2.0$ and $0° \le \theta \le 40°$. If the photoelectron energy is over 1000 eV and $\beta \approx 0$, Eq. (12) could be used for ARXPS measurement over a wide range of emission angles (0°–60°). In practical use, the IMFP and ω values are required in the MED calculations with Eq. (12). The former values can be obtained from references 12–16 or the TPP-2M predictive equation [15]. The latter values are calculated from IMFP and TMFP values obtainable from databases [26] or directly calculated from TCS [8]with Eq. (8).

4. Summary

We reported MEDs of photoelectrons excited by linearly polarized X-rays in Si, Cu, and Au over the 50 to 10,000 eV energy range. These calculations were executed for the most common experimental conditions in high-energy XPS with synchrotron radiation by employing a Monte Carlo method that uses values of electron inelastic mean free paths, λ, calculated with the relativistic full Penn algorithm and Dirac-Hatree-Fock atomic potential for elastic-scattering, as shown in Fig. 1. The calculated range of β values for MEDs were -2.0 to 2.0 (0.5 step). The resulting MED values increase as the β values decrease over the 50 to 10,000 eV energy range. We also found that the values of $D/\lambda\cos\theta$ are approximately constant to within 10% for a given value of θ and for the three elements over 1000 eV (except for the condition of β=-1) over a range of emission angles (0°– 40° with $1 \le \beta \le 2$ and photoelectron energies are over 1000 - 10 000 eV, 0° - 60°with β=0 and photoelectron energies are over 1000 - 10 000 eV). We also found that

Author Manuscript:
Published in final edited form as:
Journal of Electron Spectroscopy and Related Phenomena 190 (2013) 127–136.
https://doi.org/10.1016/j.elspec.2013.08.011

the energy dependences of the ratios $D/\lambda\cos\theta$ can be expressed by the form of Jablonski-Powell predictive equation. Finally, we have obtained a predictive MED equation [Eq. (12)] that could be applied to the wide range of experimental conditions that are used in high-energy XPS with synchrotron radiation.

5. References

[1] C.J. Powell, A. Jablonski, I.S. Tilinin, S. Tanuma, D. R. Penn, J. Electron Spectrosc. Related Phenom. 98-99 (1999) 1.
[2] C.J. Powell, A. Jablonski, J. Electron Spectrosc. Related Phenom., 178-179 (2010) 331.
[3] 18115 Surface Chemical Analysis—Vocabulary - Part 1: General terms and terms used in spectroscopy, International Organisation for Standardisation, Geneva (2010).
[4] A. Jablonski, I. S. Tilinin, and C. J. Powell, Phys. Rev. B 54 (1996) 10927.
[5] A. Jablonski, C. J. Powell, J. Vac. Sci. Technol. A 21 (2003) 274.
[6] I. S. Tilinin, A. Jablonski, J. Zemek, and S. Hucek, J. Electron Spectrosc. Relat. Phenom. 87 (1997)127.
[7] A. Jablonski, Surf. Sci., 586 (2005) 115.
[8] F. Salvat, A. Jablonski, C.J. Powell, Computer Physics Communications 165 (2005) 157.
[9] M. B. Trzhaskovskaya, V. I. Nefedov, and V. G. Yarzhemsky, Atomic Data and Nuclear Data Tables, 77 (2001) 97.

[10] M. Novak, N. Pauly, and A. Dubus, J. Electron Spectrosc. Related Phenom. 185 (2012) 4.

[11] Japanese Chemical Scociety Ed., "Electron Spectroscopy (in Japanese)", Gakkai syuppann-sennta, Tokyo (1977) P62.
[12] H. A. Bethe, Handbuch der Physik, Vol. 24, Springer-Verlag, Berlin, 1933, p. 483; H. A. Bethe, E. E. Salpeter, "Quantum Mechanics of One- and Two-Electron Atoms," Academic Press, New York(1957) Sec. 69.

[13] S. Tanuma, C. J. Powell, D. R. Penn, Surf. Interface Anal.,11 (1987) 577.
[14] S. Tanuma, C. J. Powell, D. R. Penn, Surf. Interface Anal.,17 (1991) 911.
[15] S. Tanuma, C. J. Powell, D. R. Penn, Surf. Interface Anal.,17 (1991) 929.
[16] S. Tanuma, C. J. Powell, D. R. Penn, Surf. Interface Anal.,21 (1994)165.
[17] S. Tanuma, C. J. Powell, D. R. Penn, Surf. Interface Anal.,43 (2011) 689.
[18] H. Shinotsuka, S. Tanuma, C. J. Powell, D.R. Penn, Nucl. Instrum. Methods Phys. Res. B 270 (2012) 75.
[19] A. Jablonski, Surf. Science 188 (1987) 164.
[20] A. Jablonski, H. Ebel, Surf. Interface Anal. 11 (1988) 627.
[21] A. Jablonski, Surf. Interface Anal. 15 (1990) 559.

Author Manuscript:
Published in final edited form as:
Journal of Electron Spectroscopy and Related Phenomena 190 (2013) 127–136.
https://doi.org/10.1016/j.elspec.2013.08.011

[22] H. Shinotsuka, H. Arai, T. Fujikawa, Phys. Rev. B, 77 (2008) 085404
[23] A. Jablonski, C. J. Powell, J. Vac. Sci. Technol. A27 (2009) 253.
[24] I. S. Tilinin, A. Jablonski, J. Zemek, and S. Hucek, J. Electron Spectrosc.Relat. Phenom. 87 (1997)12.
[25] A. Jablonski and S. Tougaard, Surf. Sci. 432 (1999) 211.
[26] A. Jablonski, F. Salvat, and C. J. Powell, NIST ELECTRON ELASTICSCATTERING CROSS-SECTION DATABASE, Version 3.1, Standard Reference Data Program Database 64, U.S. Department of Commerce, National Institute of Standards and Technology, Gaithersburg, MD, 2003 http://www.nist.gov/srd/nist64.htm.

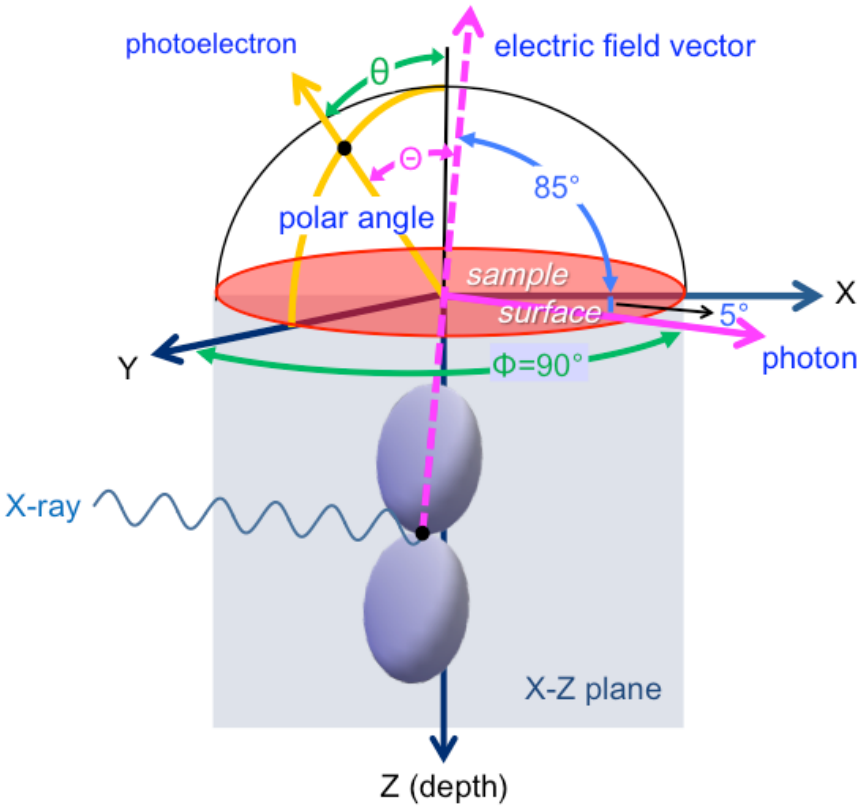

Fig. 1. Schematic diagram of the experimental configuration for Monte Carlo calculations of the emission depth distribution function.

Author Manuscript:
Published in final edited form as:
Journal of Electron Spectroscopy and Related Phenomena 190 (2013) 127–136.
https://doi.org/10.1016/j.elspec.2013.08.011

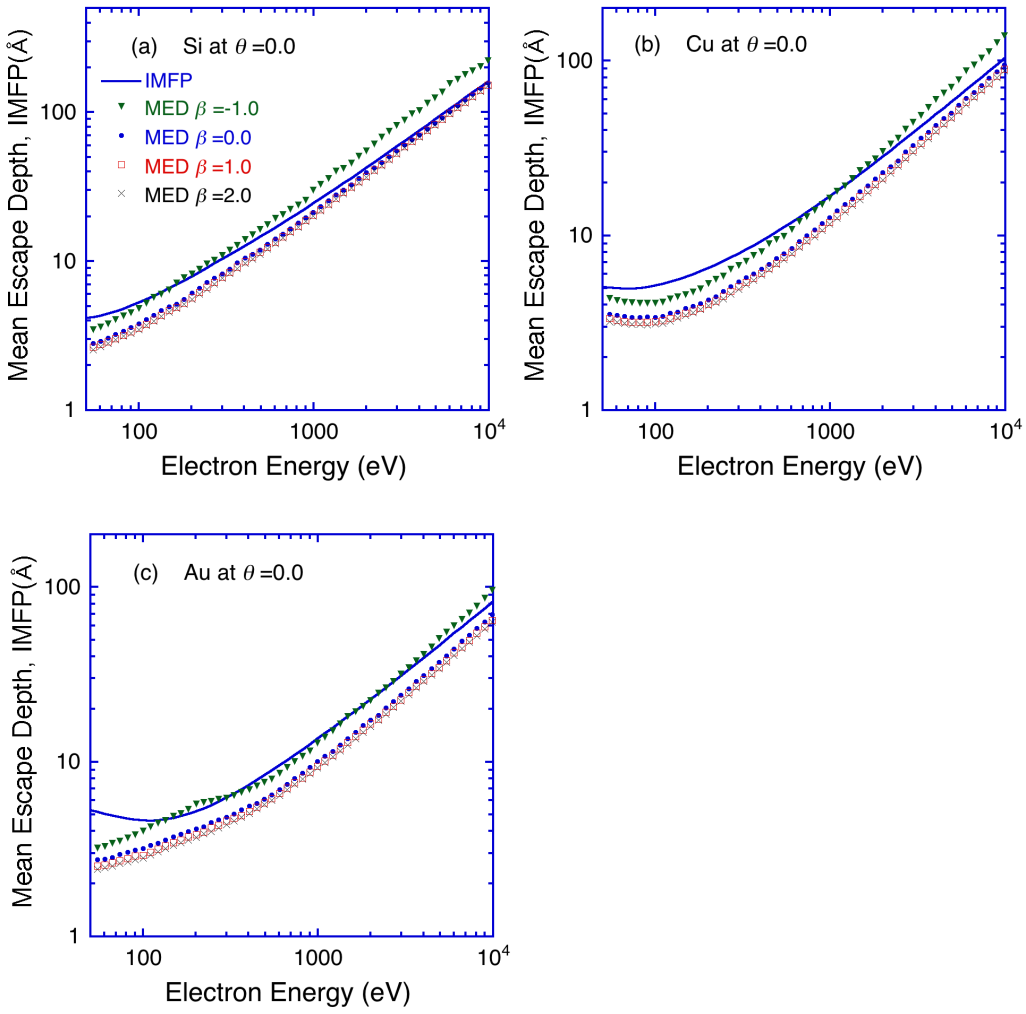

Fig. 2. MED results as a function of photoelectron energy for Si, Cu, and Au. (The emission angle, θ=0.0 with respect to the surface normal; the symmetry parameter, β =-1.0, 0.0, 1.0 and 2.0). The solid lines represent the IMFPs in the corresponding elemental solids.

Author Manuscript:
Published in final edited form as:
Journal of Electron Spectroscopy and Related Phenomena 190 (2013) 127–136.
https://doi.org/10.1016/j.elspec.2013.08.011

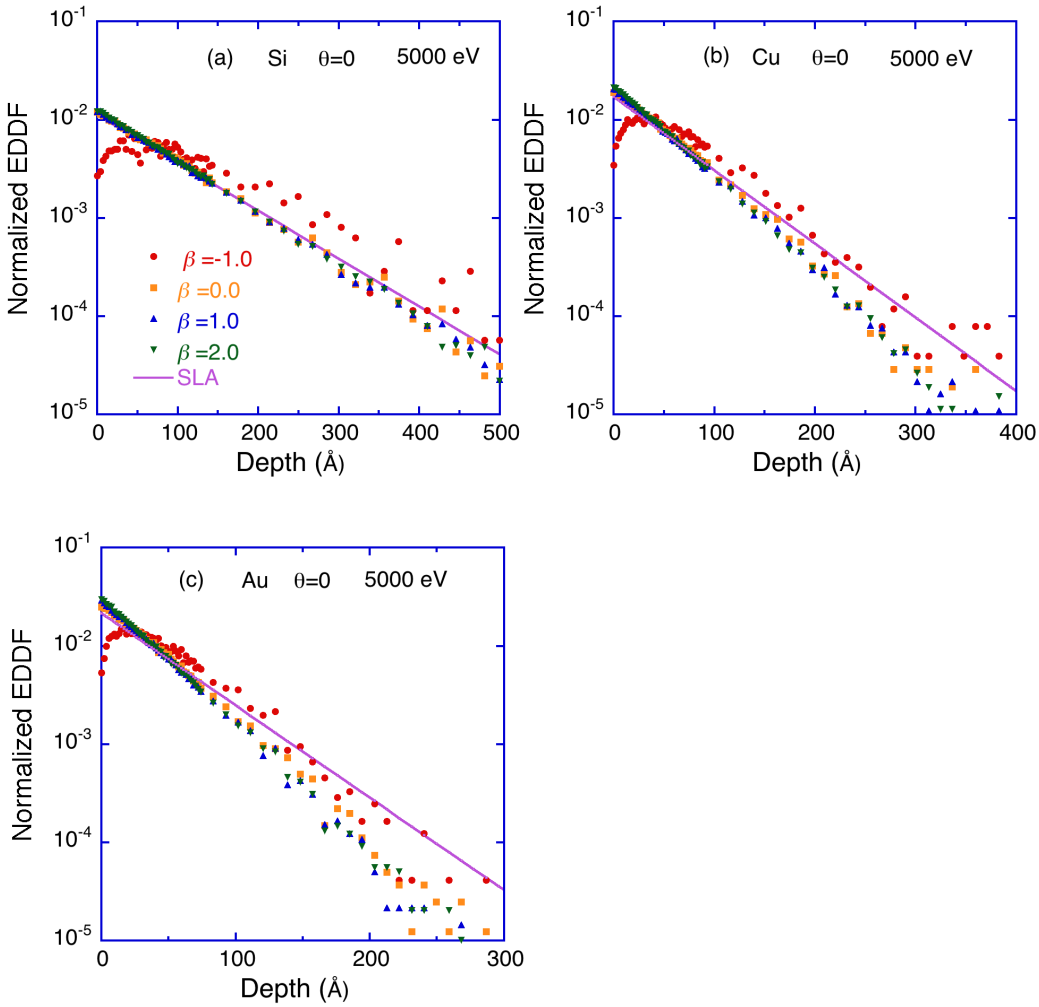

Fig. 3. Emission depth distribution functions (EDDFs) of (a) Si, (b) Cu, and (c) Au as a function of depth from the surface at photoelectron energy, E= 5000 eV; emission angle, θ= 0°; and asymmetry parameter, β= -1.0, 0.0, 1.0, and 2.0. The solid lines represent the EDDFs obtained from the SLA.

Author Manuscript:
Published in final edited form as:
Journal of Electron Spectroscopy and Related Phenomena 190 (2013) 127–136.
https://doi.org/10.1016/j.elspec.2013.08.011

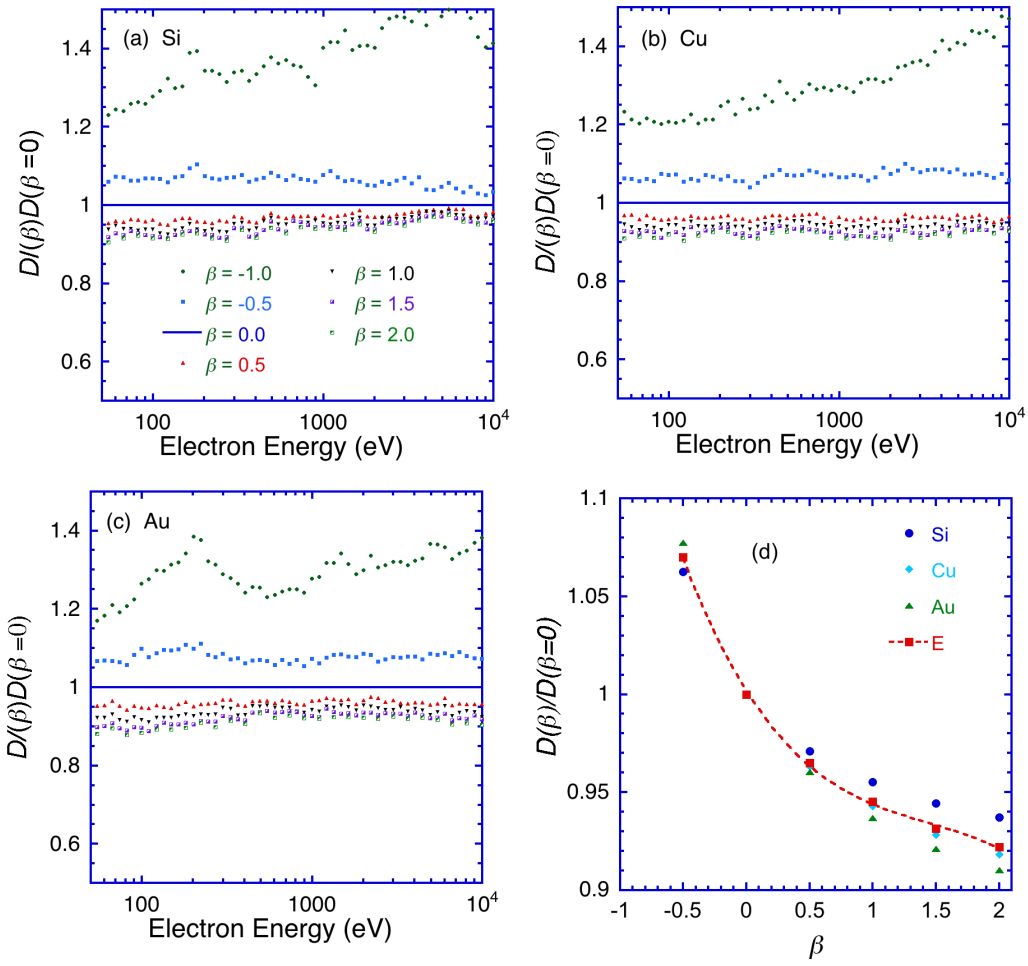

Fig. 4. MED results (shown as D values normalized to the D value with β=0.0, which corresponds to an isotropic distribution) as a function of electron energy. (a) Si, (b) Cu, (c) Au, and (d) an average of normalized MED values as a function of the asymmetry parameter, β. The dotted line shows the curve fit results with a cubic equation in (d).

Author Manuscript:
Published in final edited form as:
Journal of Electron Spectroscopy and Related Phenomena 190 (2013) 127–136.
https://doi.org/10.1016/j.elspec.2013.08.011

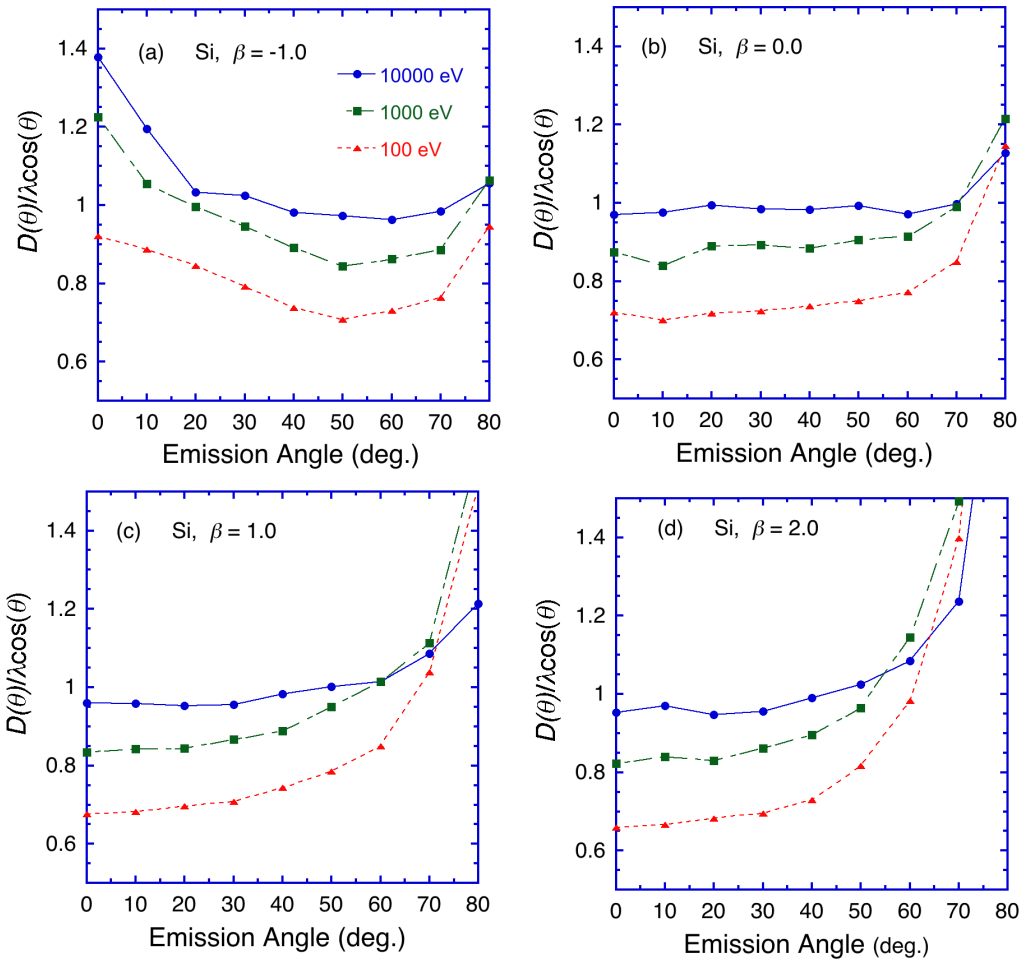

Fig. 5. MED results (shown as the ratio of D from Monte Carlo simulations to λcosθ) as a function of photoelectron emission angle for XPS with linearly polarized X-rays on Si producing 100, 1000, and 10,000 eV photoelectrons with asymmetry parameters of (a) β=-1.0, (b) β=0, (c) β=1.0, and (d) β=2.0.

Author Manuscript:
Published in final edited form as:
Journal of Electron Spectroscopy and Related Phenomena 190 (2013) 127–136.
https://doi.org/10.1016/j.elspec.2013.08.011

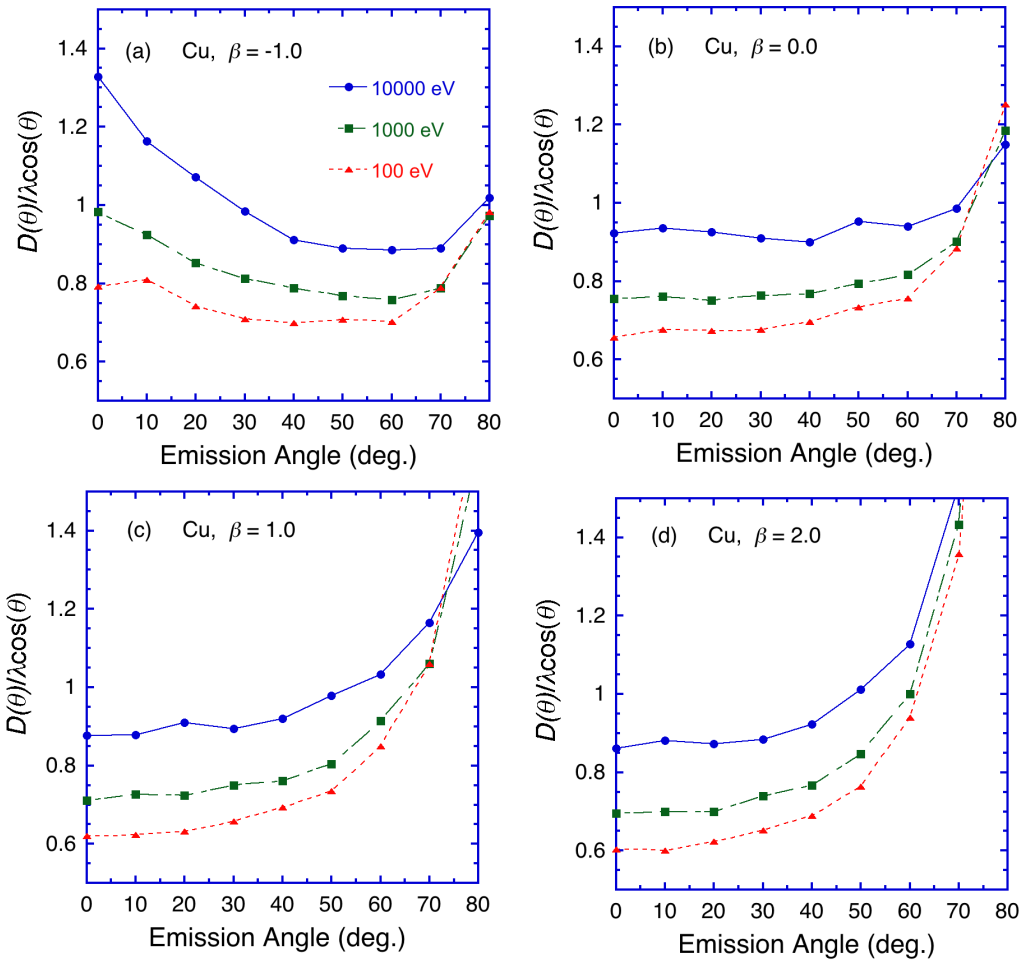

Fig. 6. MED results (shown as the ratio of D from Monte Carlo simulations to $\lambda\cos\theta$) as a function of photoelectron emission angle for XPS with linearly polarized X-rays on Cu at 100, 1000, and 10,000 eV photoelectrons with asymmetry parameters of (a) β=-1.0, (b) β=0, (c) β=1.0, and (d) β=2.0.

Author Manuscript:
Published in final edited form as:
Journal of Electron Spectroscopy and Related Phenomena 190 (2013) 127–136.
https://doi.org/10.1016/j.elspec.2013.08.011

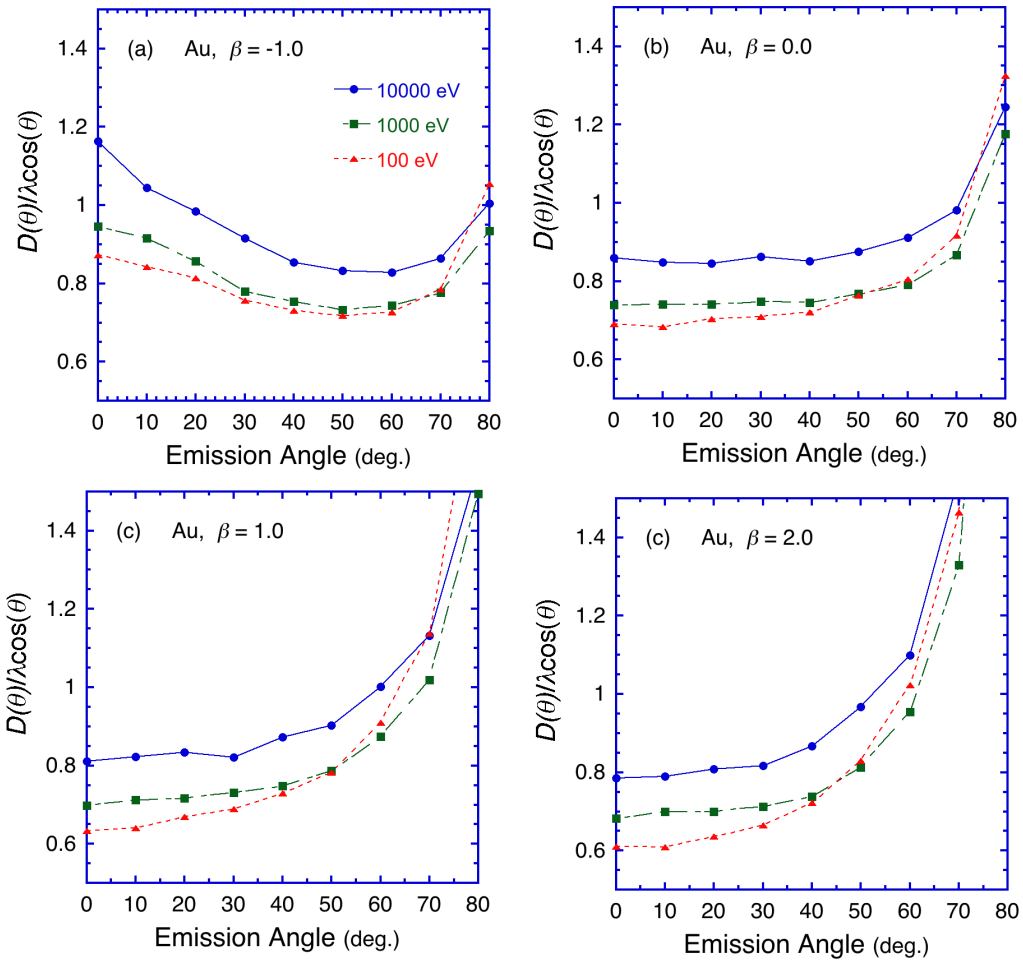

Fig. 7. MED results (shown as the ratio of D from Monte Carlo simulations to $\lambda\cos\theta$) as a function of photoelectron emission angle for XPS with linearly polarized X-rays on Au at 100, 1000, and 10,000 eV photoelectrons with asymmetry parameters of (a) β=-1.0, (b) β=0, (c) β=1.0, and (d) β=2.0.

Author Manuscript:
Published in final edited form as:
Journal of Electron Spectroscopy and Related Phenomena 190 (2013) 127–136.
https://doi.org/10.1016/j.elspec.2013.08.011

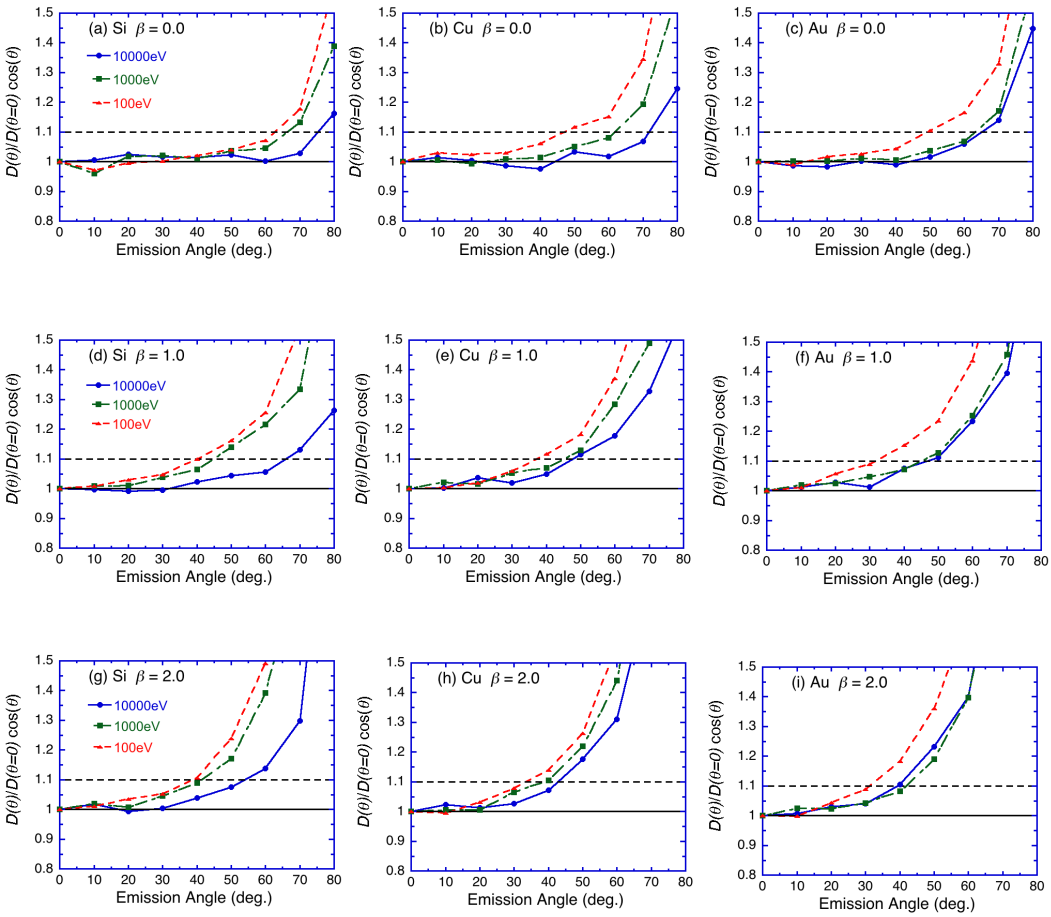

Fig. 8. Normalized MED results (shown as the ratio of $D(\theta)$ to $D(\theta=0)\cos\theta$) as a function of photoelectron emission angle for XPS with linearly polarized X-rays on Si, Cu, and Au at 100, 1000, and 10,000 eV photoelectrons with asymmetry parameters of β=0, β=1.0, and β=2.0.

Author Manuscript:
Published in final edited form as:
Journal of Electron Spectroscopy and Related Phenomena 190 (2013) 127–136.
https://doi.org/10.1016/j.elspec.2013.08.011

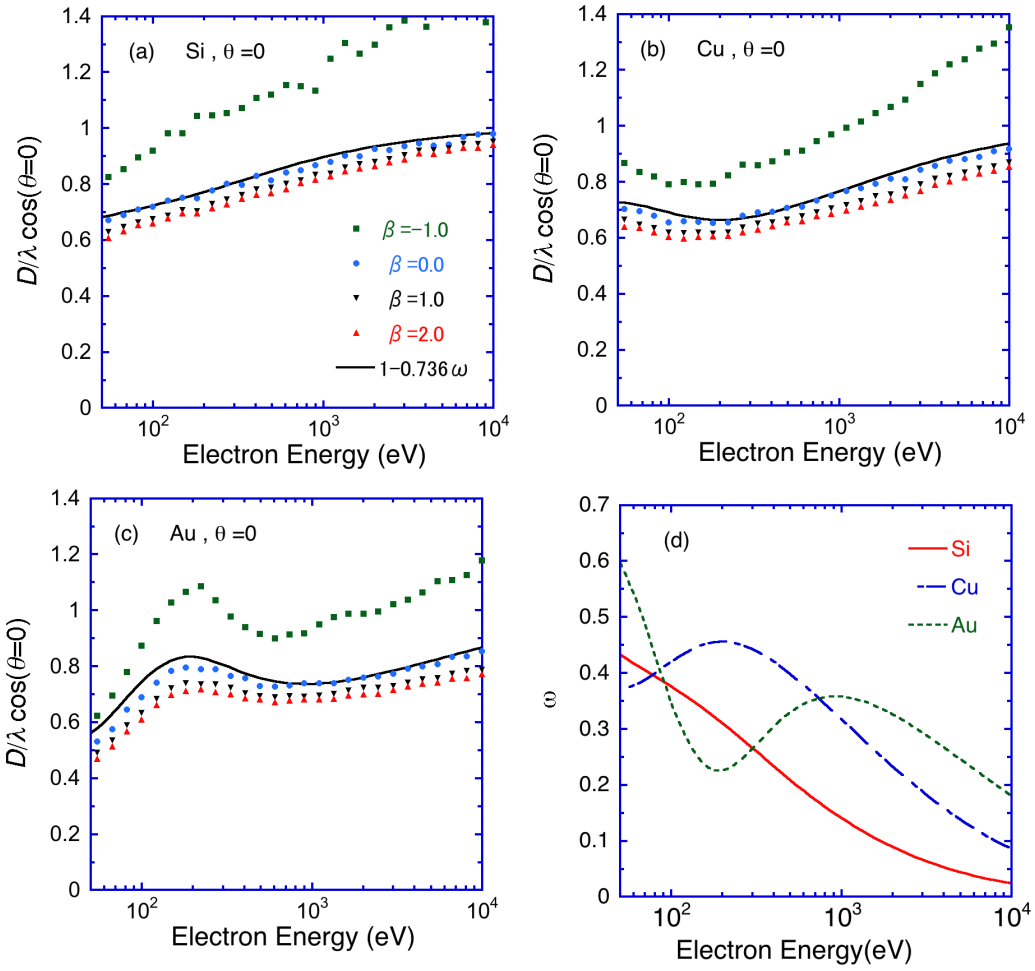

Fig. 9. MED results (shown as the ratio of D from Monte Carlo simulations to $\lambda\cos\theta$) as a function of photoelectron energy in (a) Si, (b) Cu, and (c) Au with β=-1.0, β=0, β=1.0, and β=2.0. The solid line shows the Jablonski-Powell predictive equation (D = 1 -0.736 ω). (d) Plots of the single-scattering albedo, ω, as a function of electron energy for Si ,Cu, and Au.

Author Manuscript:
Published in final edited form as:
Journal of Electron Spectroscopy and Related Phenomena 190 (2013) 127–136.
https://doi.org/10.1016/j.elspec.2013.08.011

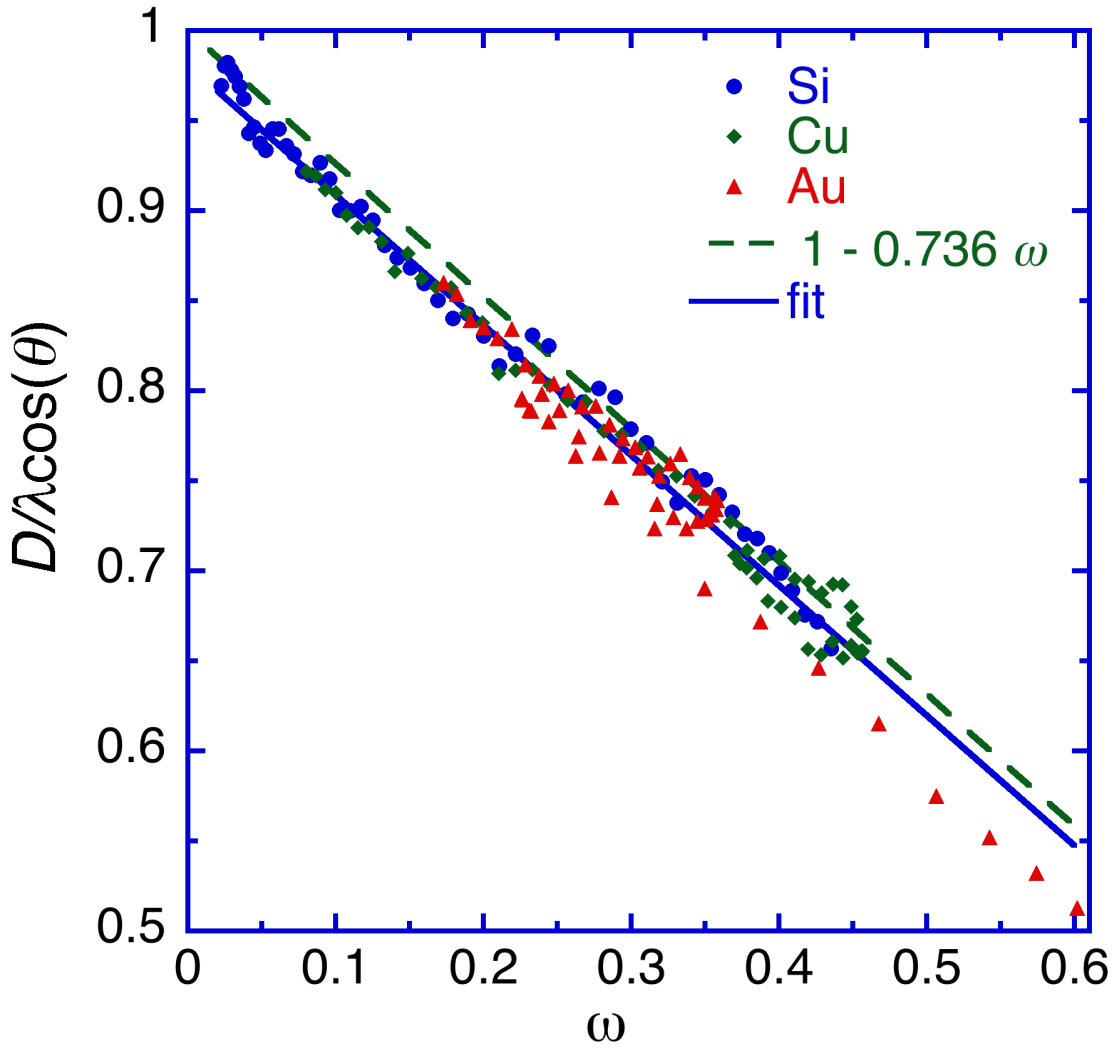

Fig. 10. Dependence of the values of the ratio of D from Monte Carlo simulations to λcosθ on the single-scattering albedo at an emission angle θ= 0° and for β=0.0. The dotted line and solid lines show the Jablonski-Powell predictive equation and the fit to the plotted points [Eq. (9)]

Author Manuscript:
Published in final edited form as:
Journal of Electron Spectroscopy and Related Phenomena 190 (2013) 127–136.
https://doi.org/10.1016/j.elspec.2013.08.011